

UNCLASSIFIED

AD 407 333

DEFENSE DOCUMENTATION CENTER

FOR

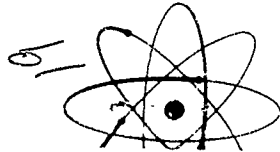
SCIENTIFIC AND TECHNICAL INFORMATION

CAMERON STATION, ALEXANDRIA, VIRGINIA



UNCLASSIFIED

NOTICE: When government or other drawings, specifications or other data are used for any purpose other than in connection with a definitely related government procurement operation, the U. S. Government thereby incurs no responsibility, nor any obligation whatsoever; and the fact that the Government may have formulated, furnished, or in any way supplied the said drawings, specifications, or other data is not to be regarded by implication or otherwise as in any manner licensing the holder or any other person or corporation, or conveying any rights or permission to manufacture, use or sell any patented invention that may in any way be related thereto.



63-4-1 AD No. **407333**

⑤ 626 600

DDC FILE COPY **1**

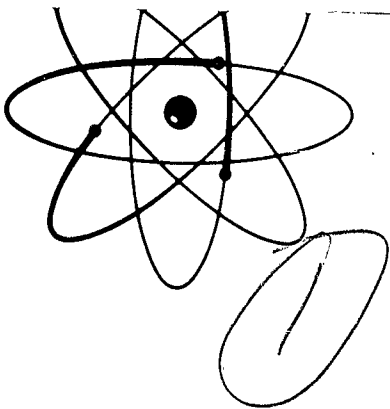
407 333



AEC (P) WP 412662
Report Number

DDC
JUN 4 1963
TISIA B

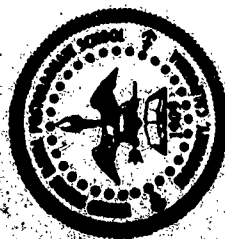
See 3



United States Atomic Energy Commission
Division of Technical Information

15-46 600

UNITED STATES
NAVAL POSTGRADUATE SCHOOL



THESIS

INVESTIGATION OF THERMAL NEUTRON
FLUX PERTURBATION IN A POLYETHYLENE
MEDIUM BY USE OF GOLD FOIL DETECTORS

by

EDWARD C. COPELAND
LIEUTENANT, UNITED STATES NAVY

and

ROGER L. REASONOVER, JR.
LIEUTENANT, UNITED STATES NAVY

1961

LIBRARY
U.S. NAVAL POSTGRADUATE SCHOOL
MONTEREY, CALIFORNIA

INVESTIGATION OF THERMAL NEUTRON
FLUX PERTURBATION IN A POLYETHYLENE
MEDIUM BY USE OF GOLD FOIL DETECTORS

Edward C. Copeland
and
Roger L. Reasonover, Jr.

LIBRARY
U.S. NAVAL POSTGRADUATE SCHOOL
MONTEREY, CALIFORNIA

⑤ 626 600

INVESTIGATION OF THERMAL NEUTRON
FLUX PERTURBATION IN A POLYETHYLENE
MEDIUM BY USE OF GOLD FOIL DETECTORS

by
Edward C. Copeland
and
Roger L. Reasonover, Jr.
Lieutenant, United States Navy
and
Lieutenant, United States Navy

Submitted in partial fulfillment of
the requirements for the degree of
MASTER OF SCIENCE
IN
PHYSICS

United States Naval Postgraduate School
Monterey, California
June 1961

INVESTIGATION OF THERMAL NEUTRON
FLUX PERTURBATION IN A POLYETHYLENE
MEDIUM BY USE OF GOLD FOIL DETECTORS

by
Edward C. Copeland
and
Roger L. Reasonover, Jr.

This work is accepted as fulfilling
the thesis requirements for the degree of
MASTER OF SCIENCE
IN
PHYSICS
from the
United States Naval Postgraduate School

William W. Hovro
Faculty Adviser

Arthur R. Fung
Chairman
Dept. of Physics

Approved:
Arthur R. Fung
Academic Dean

① ② ③ ④ ⑤ ⑥ ⑦ ⑧ ⑨ ⑩ ⑪ ⑫ ⑬ ⑭ ⑮ ⑯ ⑰ ⑱ ⑲ ⑳ ㉑ ㉒ ㉓ ㉔ ㉕ ㉖ ㉗ ㉘ ㉙ ㉚ ㉛ ㉜ ㉝ ㉞ ㉟ ㊱ ㊲ ㊳ ㊴ ㊵ ㊶ ㊷ ㊸ ㊹ ㊺ ㊻ ㊼ ㊽ ㊾ ㊿

① ②

ABSTRACT

The neutron flux perturbation in a homogeneous thermal reactor, polyethylene moderated, was investigated experimentally through use of activated gold foils of varying thicknesses. The experimental data are compared with the theoretical predictions of Bothe and Skyrme, and with the modifications introduced by Tittle and by Ritchie and Eldridge.

Experimental determination of the thermal neutron flux at the center of the core of the MGN-201 reactor indicates that Skyrme's theory and/or Skyrme's theory as modified by Ritchie and Eldridge give the best results over a range of foil thickness from two to ten mils. The greatest deviation of theoretical calculations from experimental data is less than 3%.

Determinations of other investigators for gold detectors in graphite agree to within 3% with the predictions of the Skyrme theory. In water-moderated reactors experimental determinations have been compared with the Skyrme theory as modified by Ritchie and Eldridge and found to agree to 5%.

The writers wish to express their appreciation to Professor William H. News of the U.S. Naval Postgraduate School for his patient assistance and encouragement during this investigation.

TABLE OF CONTENTS

Section	Title	Page
1.	Introduction	1
1A.	Definitions of Parameters	2
2.	Theoretical	4
3.	Experimental	10
4.	Results	14
5.	Analysis of Results	16
6.	Conclusions	21
7.	Bibliography	22
8.	Appendix I: Summary of Data	24
9.	Appendix II: Analysis of Peak-to-Total Ratio	30

LIST OF ILLUSTRATIONS

Figure	Page
1. Skyrme Function	6
2. Variational ratio for Ritchie's Equation	7
3. Flux Perturbation Correction Factors	9
4. Spectrometer Calibration Curve	11
5. Experimental Results	15
6. Comparison of Flux Depression Effects	17
7. Thermal Neutron Flux Determination	19
8. Gamma Spectrum: 2.69d Au-198	31

1. INTRODUCTION

When determining thermal neutron flux by the activation of a pure foil target, it is necessary to apply a correction for flux perturbation due to the presence of the target foil. This perturbation manifests itself in two effects:

- (a) the outside layers of the foil will absorb neutrons, thus partially shielding the inner layers, and
- (b) absorption of neutrons by the foil depletes the number of neutrons in the diffusion medium around the foil.

The net result is a depression in the flux. That is, the flux level as seen by the foil is decreased below its normal value.

Bothe (1) considered the problem of neutron flux perturbation using first-order diffusion theory. His results were later modified by Tittle (2,3). Subsequently, the problem was attacked by Skyrme (4) utilizing the one-speed transport theory. Most recently, Ritchie and Eldridge (5) have discussed both approaches and proposed a refinement to the Skyrme theory as being most appropriate.*

The present investigation presents experimental data for flux variation in a polyethylene-moderated medium. In order to extrapolate these measurements to the unperturbed flux it is necessary to examine the several theories. Comparisons with experiment have not been particularly successful in deciding between theories. However, it might appear that the most reliable value for the unperturbed flux would be given by that showing the best agreement.

* Since the inception of this investigation, Dalton and Osborn (16) have proposed a theory which converts the transport equation to an iterative integral equation which is then solved by computer methods. Comparison of the experimental results with their approach is not included in this investigation.

1A DEFINITIONS

(Numerical values indicated below apply to this investigation.)

- d - foil thickness in cms.
- Σ_{af} - macroscopic cross-section for absorption of thermal neutrons in the foil (5.19 cms.⁻¹)
- x - $d \Sigma_{af}$
- r - foil radius (0.635 cms)
- $E_3(x)$ - the exponential integral of the third order = $\int_0^x \frac{e^{-y}}{y^3} dy$
- λ_s - the scattering mean free path of the diffusion medium (0.625 cm)
- λ_{tr} - the transport mean free path of the diffusion medium

$$\lambda_{tr} = \frac{\lambda_s}{1 - \cos 0} \quad (0.731 \text{ cm})$$

- $\cos 0$ - the average value of the cosine of the scattering angle (0.143)
- λ_t - total mean free path of the diffusion medium (0.616 cm)
- L - diffusion length of the diffusion medium (2.315 cm)
- $R^0(x)$ - the absolute disintegration rate of the foil after irradiation
- μ - gamma mass absorption coefficient for gold (0.19 cm²/gm)
- m - mass of the foil in grams
- w - atomic weight of the foil (198)
- N_0 - Avogadro's Number
- σ^0 - thermal absorption cross-section for gold at 0.0253 ev (98.8 barns)
- σ_a - the average thermal absorption cross-section for the foil
- T - total time of irradiation of the foil in minutes
- t - elapsed time between irradiation and counting, in minutes
- λ - the decay constant for Au-198 (1.70 x 10⁻⁴ min.⁻¹)
- Σ_a - macroscopic absorption cross-section of the diffusion medium (0.0233 cm⁻¹)
- γ' - the ratio of the scattering cross-section to the total cross-section of the diffusion medium (0.986)

- ϕ_t - the average observed thermal neutron flux
- ϕ_0 - the total thermal neutron flux in the undisturbed medium
- $F = \frac{\phi_t}{\phi_0}$ Subscripts: B signifying Bothe, T - Tittle, S - Skyrme, and R - Ritchie
- N_p - measured number of events per second occurring under the photopeak
- f_e - detector efficiency (0.118 at a sample-to-detector distance of three cms)
- f_s - gamma self-absorption correction
- f_{ic} - factor for internal conversion (0.96)
- R_{pt} - the peak-to-total ratio (0.725)

2. THEORETICAL

Bothe's theory for perturbation of thermal flux by a target foil, based on first-order diffusion theory, assumes the following:

- (1) a medium of infinite extent containing a uniformly distributed source,
- (2) one-speed isotropic laboratory scattering, and
- (3) a foil which is a pure absorber.

His expression is:

$$\Phi_B = \frac{\left[\frac{1}{2} - \frac{R(x)}{3} \right] 1/x}{1 + \left[\frac{1}{2} - \frac{R(x)}{3} \right] \cdot g_B} \quad (1)$$

where g_B is given by one of the following equations:

$$g_B = \left[\left(\frac{x}{\lambda_s} \right) \left(\frac{-3L}{2x + 3L} \right) - 1 \right] \quad \text{for } x \gg \lambda_s$$

$$g_B = 0.46 \frac{x}{\lambda_s} \quad \text{for } x \ll \lambda_s$$

Tittle concluded that the above Equation (1) was basically correct; however, he felt that the accuracy of the expression was increased by use of the transport mean free path rather than the scattering mean free path. He gives, replacing g_B in Equation (1):

$$g_T = \left[\left(\frac{3x}{2\lambda_{tr}} \right) \left(\frac{-L}{x + L} \right) - 1 \right] \quad \text{for } x \gg \lambda_{tr}$$

$$g_T = 0.68 \frac{x}{\lambda_{tr}} \quad \text{for } x \ll \lambda_{tr}$$

Skyrme approached the perturbation problem using one-speed transport theory, involving a transport theory calculation of the neutron flux in the medium evaluated at the position of the foil and averaged over its

surface. The basic assumptions concerning the isotropic field are the same as Bothe's. Skyrme's original equation has been transformed by Ritchie and Eldridge to give a relation of the same form as Equation (1):

$$\Phi_S = \frac{\left[\frac{1}{2} - \frac{R_3(x)}{3} \right] 1/x}{1 + \left[\frac{1}{2} - \frac{R_3(x)}{3} \right] \cdot g_S} \quad (II)$$

$$\text{where } g_S = \frac{3L}{2\lambda_c} \cdot S \left(\frac{2x}{L} \right)$$

$$\text{and } S \left(\frac{2x}{L} \right) = 1 - \frac{4}{\pi} \int_0^1 \sqrt{1 - \xi^2} e^{-\frac{2x}{L}\xi} d\xi$$

defined as the Skyrme Function. (Figure 1)

Ritchie and Eldridge proposed further that the flux depression is represented better in the general case of a foil of finite dimensions if g_S is multiplied by the ratio $\left[\frac{g_v}{g_S} \right]$ which is presented graphically in figure 2. Therefore,

$$g_R = g_S \left[\frac{g_v}{g_S} \right]$$

Essentially, the numerator of Equation (II) gives the correction for the foil "self-protection" effect while the denominator corrects for the neutron depression in the diffusion medium due to absorption. The foil radius, the size of which is dictated by the physical dimensions of the reactor access, is comparable with λ_s and λ_{tr} in this investigation, necessitating a choice of formula for the computation of g_S and g_T . Preliminary computations and comparisons with experimental data indicated that the formula for $x \ll \lambda$ are most nearly valid. This difficulty does not arise in g_S or g_R .

The computed values of the g-factors are listed in Table I* together with total flux depression ratios as given by the several theories. The

Figure 1

Skyrme
Function (5)

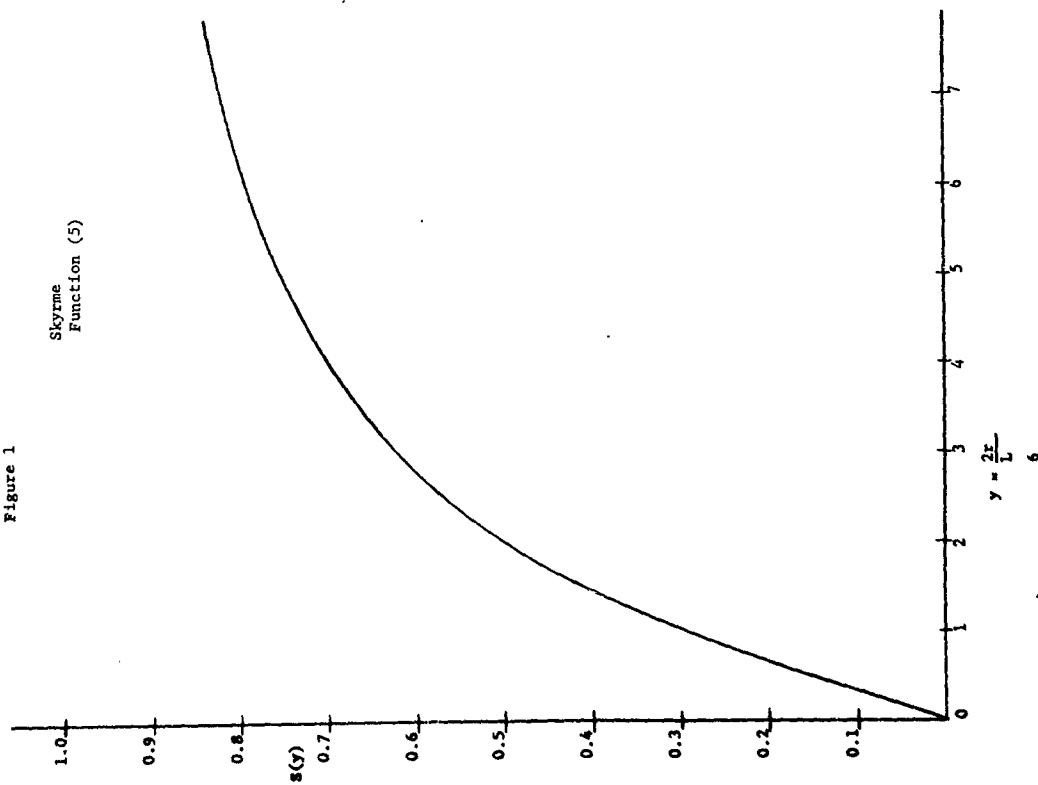
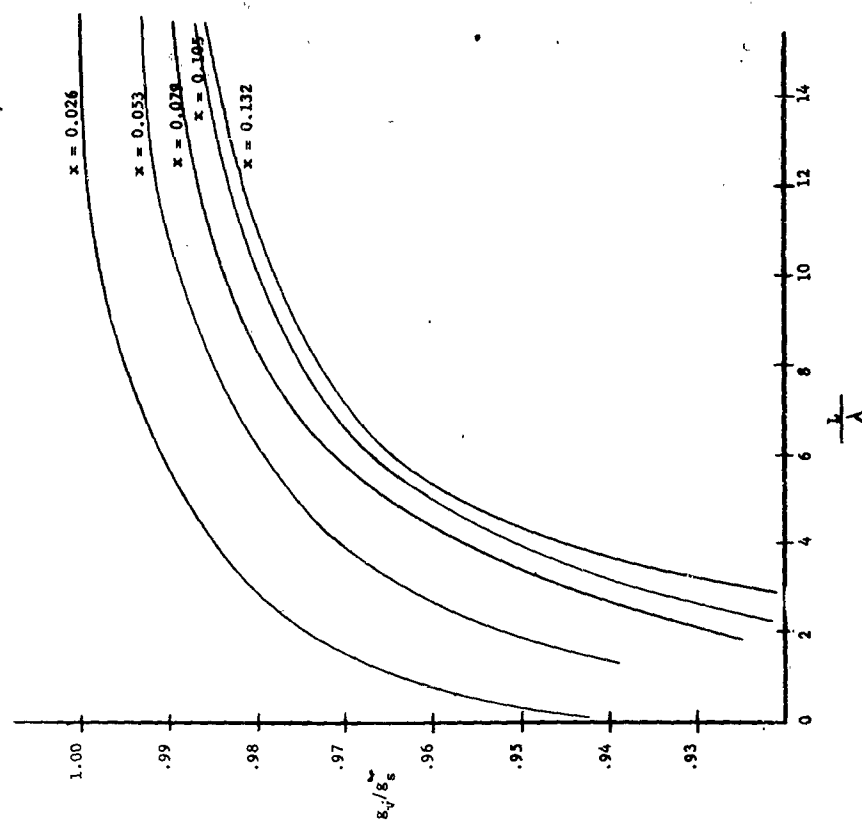


Figure 2

Variational Ratio
for
Ritchie's Equation (5)



flux depression ratios are also presented graphically in Figure 3.

Table I

d (mils)	x	g_B	g_T	g_S	g_R	F_B	F_T	F_S	F_R
2	.0264	.467	.592	1.122	1.104	.927	.925	.913	.914
4	.0527				1.087	.878	.873	.852	.854
6	.0791				1.071	.834	.828	.800	.803
8	.1055				1.064	.798	.790	.757	.760
10	.1319				1.056	.765	.755	.717	.722

* The values of the third-order exponential integral, $E_3(x)$, used in these calculations were obtained from Case, et al (22).

Theoretical determination
of Thermal Neutron Flux
Perturbation in Circular
Gold Foils of .50 inch
diameter

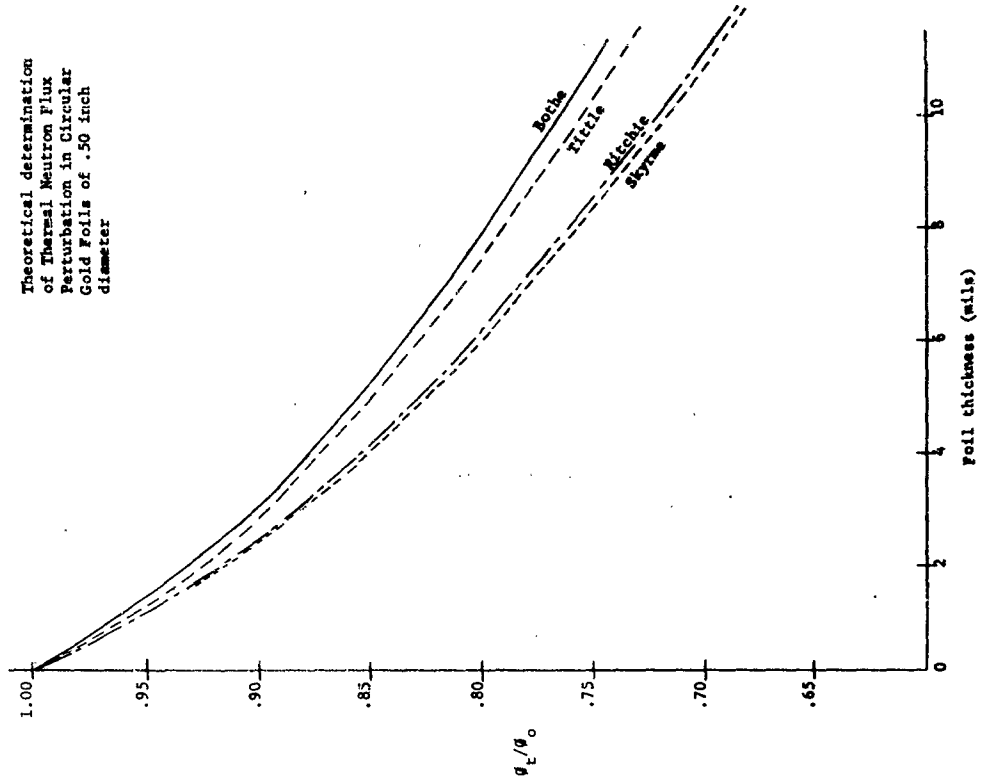
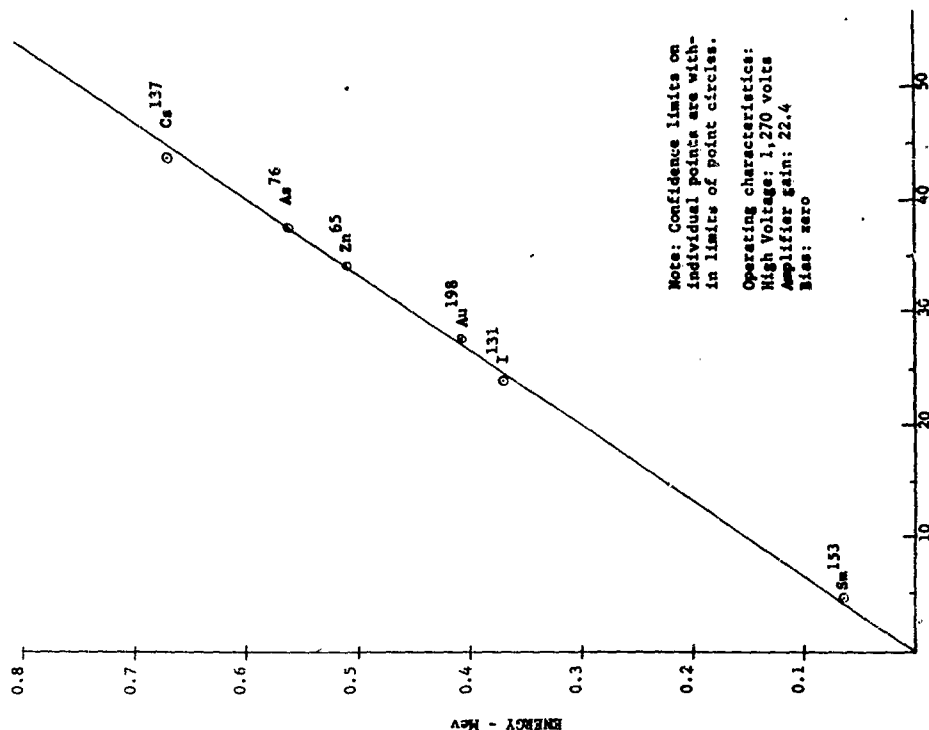


Figure 3

SPECTROMETER CALIBRATION CURVE



Note: Confidence limits on individual points are within limits of point circles.
Operating characteristics:
High Voltage: 1,270 volts
Amplifier gain: 22.4
Bias: zero

CHANNEL NUMBER
Figure 4
11

3. EXPERIMENTAL

Circular gold foils of 0.50 inch diameter were compounded in increments of two mils to provide a range of thicknesses from two to ten mils. These foils were mounted at the center axially and longitudinally of a ten-inch cylindrical polyethylene rod of 0.80 inch diameter which, in turn, filled the glory hole of the AGN-201 reactor. Thus each foil was irradiated at the center of the reactor core. The power level was the same for each irradiation to within 1%. Time of irradiation was accurate to within one minute. Radiation times were adjusted so that the activity of each foil was approximately the same. Placement of the foil was accurate to within one millimeter, and the mass of the foil was determined to ± 0.1 mg.

The absolute disintegration rate of the foils was determined by use of a Tracerlab MLP-6 Step-Scanning Spectrometer equipped with a 3" diameter by 3" thick Harshaw type 12A12 Thallium-activated Sodium Iodide crystal mounted on a D-mount type 6363 photomultiplier tube. The scanner was calibrated to provide fifty equal increments from 0 to 0.75 Mev (6). The calibration data are given in Table II and plotted in Figure 4. The curve is to within 1.0% standard deviation from the mean. The calibration was checked daily for drift which was found to be less than 1%, but since the determination involved only the use of the photopeak, any drift in the spectrometer would not appear in the final results.

Table II

Isotope	Calibration Data	
	Gamma Energy Kev	Channel
Sm-153	69.0	4.82
I-131	364.0	24.58
Au-198	411.8	27.71
Zn-65	511.0	34.10
Au-76	560.5	37.55
Cs-137	662.6	43.58
	Mean:	14.85 \pm 0.13
		10

The foils were mounted for counting on a 0.054 inch thick plexiglass tray at a sample-to-crystal distance of three cms. The tray was of adequate thickness to reduce beta radiation to an insignificant amount. The sample tray was mounted in a plastic holder which, together with the NaI crystal and photomultiplier tube, was mounted inside a lead shield as described by Clements and Kelly (6). By this arrangement the backscatter was less than 4% of the total measured activity. Figure 8 (Appendix II).

The absolute disintegration rate was calculated from the measured activity by the relation:

$$R^0(x) = \frac{N_p}{f_c \cdot f_{ic} \cdot R_p \cdot (1 - \exp[-\lambda T]) \cdot \exp(-\lambda t)} \quad (II)$$

The total number of events per second under the photopeak, N_p , was computed following the method of Clements and Kelly (6). The values for crystal detection efficiency and peak-to-total ratio are 0.118 and 0.725, respectively, as determined by Heath (7,8). The value of the internal conversion factor is given by Raffle (9) as 0.96. Sola (10) gives the following equation for self-absorption in the foil:

$$f_s = \frac{1 - \exp(-\lambda d)}{\lambda d}$$

Cooke (11) calculated the spectral-hardening effect in the AGN-201 reactor which results in an effective thermal energy of 0.0296 ev vice the accepted 0.0253 ev. Employing the technique of Meadows (12) and Westcott (13), an average effective thermal cross-section for this value of thermal energy was calculated and found to be 88.3 barns. Clements and Kelly (6) found a Cadmium ratio for this reactor to be 5.36, which gives a ratio of thermal activations in the foil to total activations equal to 0.815. This ratio will not be constant over the entire range of foil thicknesses, but the error may be neglected as it is less than 1%.

at its maximum value (13). The average flux in the foil may then be calculated in the conventional manner using the expression:

$$\phi_t = \frac{0.815 R^0(x) W}{N_0 \sigma_a m} \quad (III)$$

For each foil thickness, three separate determinations were made; in each determination the foil was counted three times giving nine values of $R^0(x)$ for each increment of thickness between two and ten mils. Counting procedures insured statistical precision to within 1%. The experimental data obtained are given in Table III with the maximum deviation for each thickness.

Table III

d (mils)	N_p (counts/sec)	$R^0(x)$ (counts/sec)	ϕ_t (neut/cm ² sec)	ϕ_t (max deviation)
2	2.87×10^4	1.41×10^5	3.43×10^6	-0.15×10^6
4	2.36×10^4	2.61×10^5	3.19×10^6	$+0.11 \times 10^6$
6	2.27×10^4	3.62×10^5	2.94×10^6	$+0.12 \times 10^6$
8	2.20×10^4	4.25×10^5	2.59×10^6	$+0.08 \times 10^6$
10	2.47×10^4	5.04×10^5	2.46×10^6	-0.27×10^6

The thermal neutron flux in the undisturbed medium, ϕ_0 , is given by:

$$\phi_0 = \frac{\phi_t}{F} \quad (IV)$$

where F is the appropriate theoretical correction factor as listed in Table I.

4. RESULTS

The nine experimental determinations of θ_t for each foil thickness were averaged in accordance with standard statistical procedures. The mean values and their standard deviations are given in Table IV. Values of θ_o were calculated from the various theories using the factors listed in Table I; these are shown in the last four columns of Table IV. It is evident that a constant value for θ_o is not obtained in any case.

Table IV

d (mils)	$\theta_t \times 10^6$ (neut/cm ² sec)	Standard error for θ_t	$\theta_o \times 10^6$ (neut/cm ² sec)			
			Bothe	Tittle	Skyrme	Ritchie
2	3.43	0.03	3.70	3.71	3.76	3.75
4	3.19	0.03	3.63	3.65	3.74	3.74
6	2.94	0.03	3.53	3.55	3.68	3.66
8	2.59	0.02	3.25	3.28	3.42	3.41
10	2.46	0.07	3.22	3.26	3.43	3.41

Figure 5 shows the experimental data fitted to a straight line by the "least squares" procedure. The straight-line fit is consistent with the experimental results of other investigators. Zobel (14) has made a rather precise and exhaustive investigation into water-moderated systems through gold foil exposure. His results show that, for the range from one to ten mils, the plot of thermal flux versus foil thickness is indeed a straight line within the limits of experimental accuracy. Bach (15) has determined that the binding effects on the neutron spectra will be quite similar for polyethylene and water molecules, differing by a maximum of ~15%. Therefore, the perturbation curves should be similar in appearance, which justifies the straight line interpretation of the experimental curve in Figure 5.

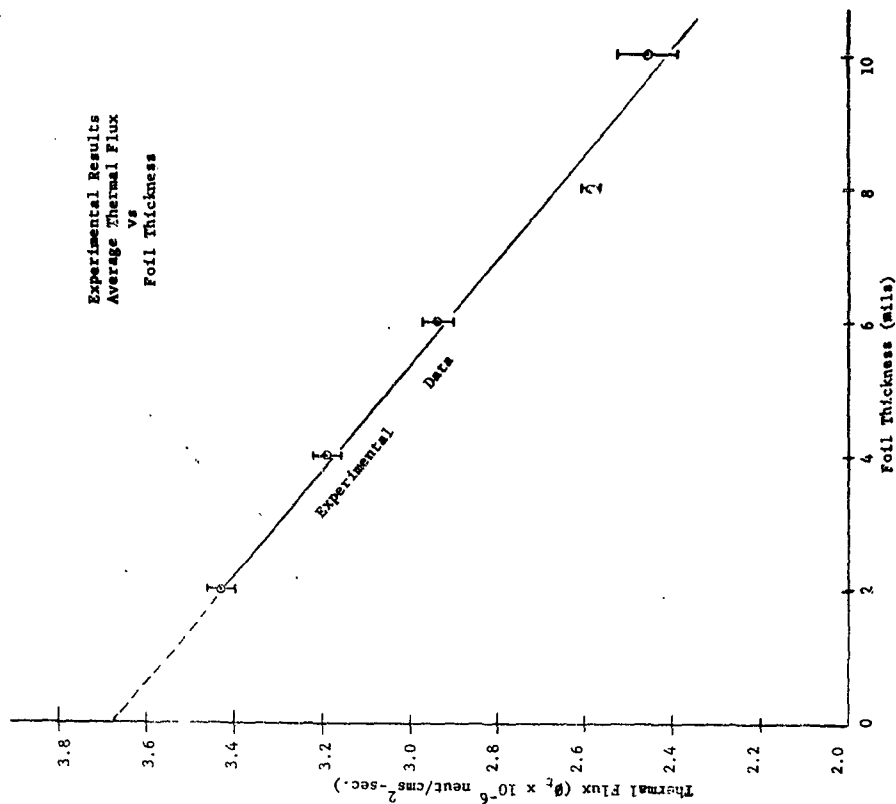


Figure 5

5. ANALYSIS OF RESULTS

Ritchie and Eldridge (5) proposed a method of analysis which, in essence, consist of comparing the various factors for flux depression effect only.

Equation III may be written:

$$\phi_t = \frac{0.815 E_0(x)}{\pi r^2 x} \quad (V)$$

and:

$$F = \frac{\phi_t}{\phi_0} = \frac{\left[\frac{1}{2} - E_3(x) \right] \frac{1}{x}}{1 + \left[\frac{1}{2} - E_3(x) \right] g} \quad (VI)$$

Substituting Equation (V) for ϕ_t in Equation (VI) and rearranging:

$$1 + \left[\frac{1}{2} - E_3(x) \right] g = \frac{c \left[\frac{1}{2} - E_3(x) \right]}{R^0(x)} \quad (VII)$$

where c is a constant of proportionality.

From Equation (VII), it is easily shown that the zero thickness intercept, multiplied by c , must equal one. Before the data can be plotted, for comparison, it is necessary that they be normalized consistent with the intercept value. To do this, c was evaluated for the two thinnest foils by each of the theoretical treatments. The values so obtained varied from 5.64×10^6 to 5.82×10^6 with a mean of $5.76 \pm .08 \times 10^6$ *

* From the equations involved, c is also seen to be equal to $\phi_0 \pi r^2 / 0.815$; however, this relation cannot be employed for a reliable evaluation of ϕ_0 . For comparison with final results, this relationship yields a value of $\phi_0 = 3.70 \times 10^6$ neut/cm² sec.

Figure 6

Comparison of Flux Depression
with Experimental Data.

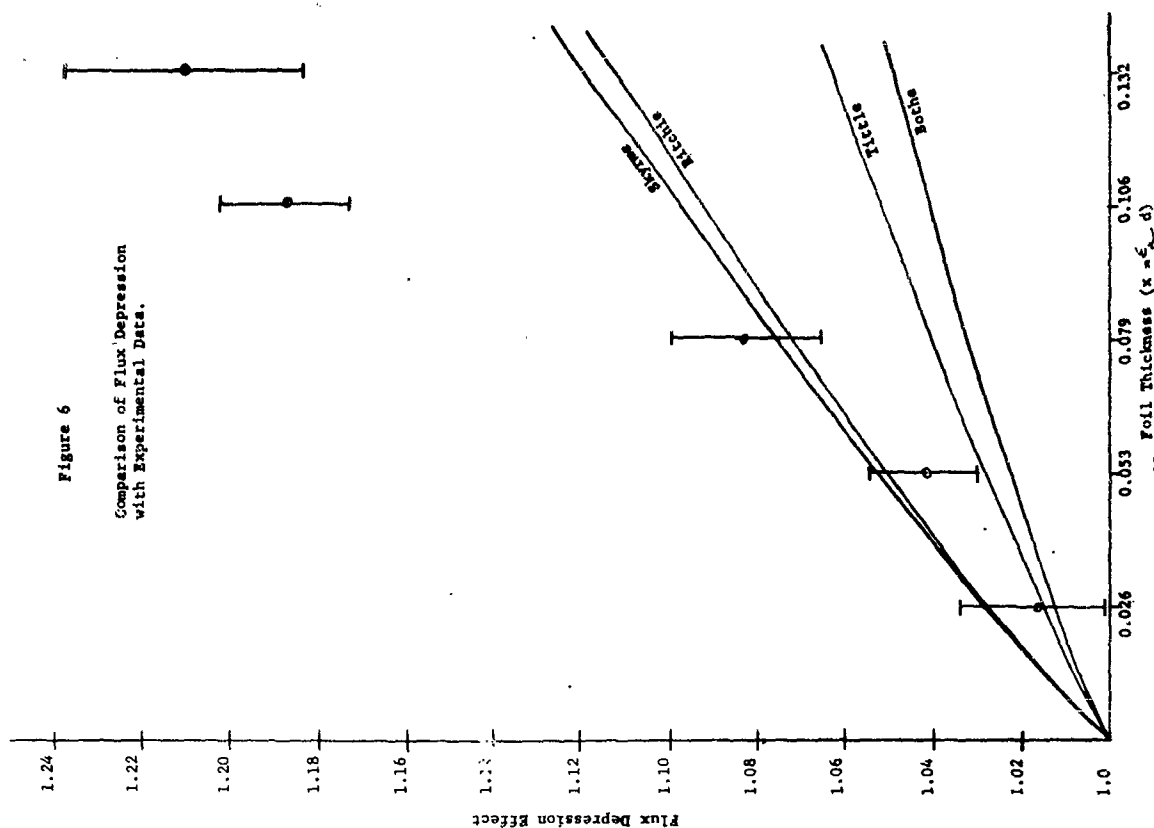


Figure 6 is a plot of $c [1/2 - E_3(x)] / R^0(x)$ versus foil thickness along with the theoretical values of $1 + [1/2 - E_3(x)] g$. The values for the various thicknesses are given in Table V.

Table V

x	$1 + [1/2 - E_3(x)] g$		$R^0(x)$ ($\times 10^5$ c/sec)	$c [1/2 - E_3(x)]$ $R^0(x)$
	Bothe	Little Skyrme Ritchie		
0.0264	1.012	1.028	1.027	1.406
0.0528	1.022	1.028	1.051	2.612
0.0792	1.032	1.040	1.073	3.618
0.1056	1.041	1.052	1.093	4.249
0.1320	1.049	1.063	1.112	5.036
			1.210	

Figure 6 shows that there is actually little difference between the results of Skyrme and Ritchie and that our results more closely approximate these predictions, particularly at small foil thicknesses. Indeed, only the single determination at 2 mils is, within estimated error, in agreement with Little or Bothe. It appears that either of the first two might be used to extrapolate to zero thickness. In view of the approximate character of Ritchie and Eldridge's second correction, the g_0/E_0 multiplier to g_s , the data have been extrapolated using g_s .

Equation (IV), rearranged, gives: $\theta_t = \theta_0 F$ which is the equation of a straight line, whose slope is θ_0 , and whose end-points are at the origin and at $F = 1$ where $\theta_t = \theta_0$. A plot of θ_t versus F , for the five experimentally determined values of thermal flux plus the origin as a necessary sixth point should give the best possible determination of θ_0 . In Figure 7 the data are plotted in this manner with the straight line being fitted by the procedure of "least squares". This yields from the value of θ_t at

$$F_s = 1:$$

$$\theta_0 = 3.64 \times 10^6 \text{ neutrons/cm}^2 \cdot \text{sec.}$$

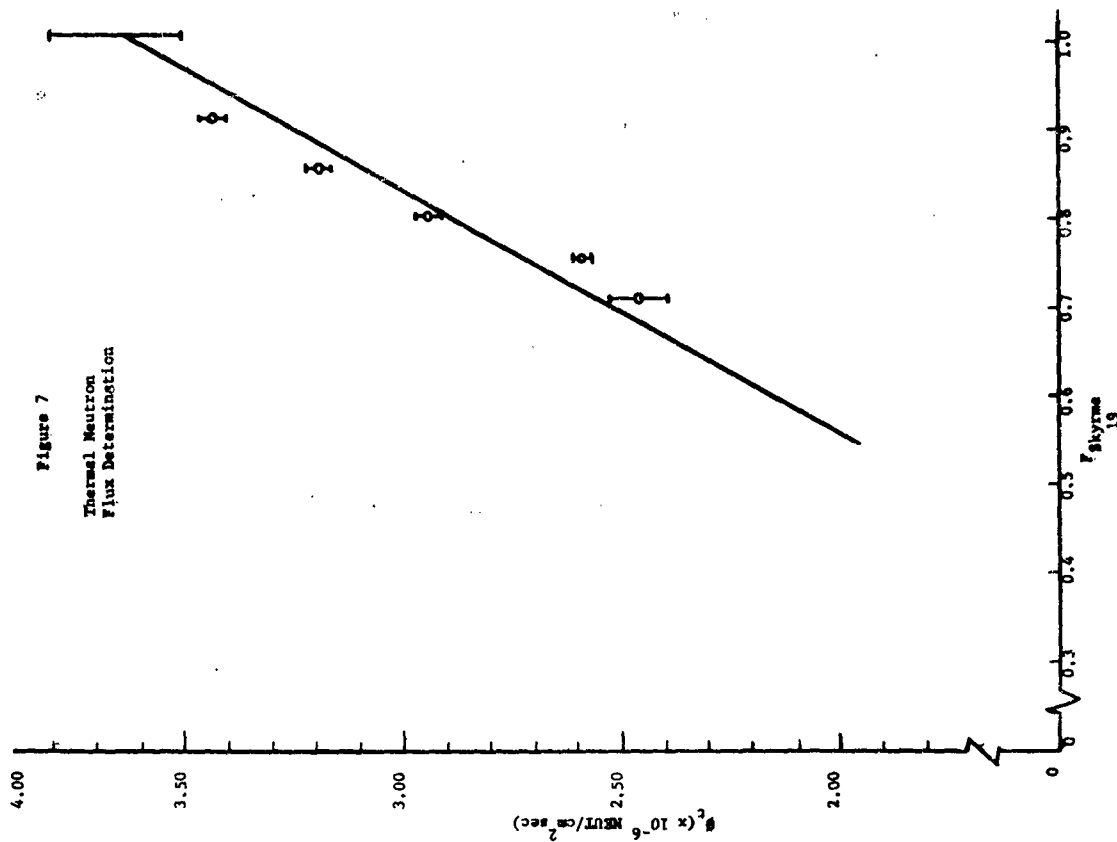


Figure 7
Thermal Neutron
Flux Determination

and from the slope:

$$\dot{\phi}_0 = 3.68 \times 10^6 \text{ neutrons/cm}^2 \text{ - sec.}$$

Their mean value is 3.66×10^6 which is also the value to which $\dot{\phi}_t$ extrapolates linearly to $x = 0$ (Figure 5). From a consideration of all factors (including counting statistics, geometry of counting, errors in irradiation power level, etc.) it is estimated that the statistical precision is within $\pm 5\%$.

6. CONCLUSIONS

- (1) $\dot{\phi}_0 = 3.66 \pm 0.18 \times 10^6$ neutrons/cm² - sec.
- (2) From this investigation, it is not possible to give preference to either Skyrme's or Ritchie's method of flux perturbation calculation in a polyethylene diffusion medium; however, either is more nearly correct than Rothe's and Tittle's calculations.
- (3) A very good value of $\dot{\phi}_0$ may be obtained by determining a number of values of $\dot{\phi}_t$ between two and ten mils, and using a straight line extrapolation to zero thickness.

BIBLIOGRAPHY

1. W. Bothe, Zur Methodik der Neutronensonden, Z. Physik 120, 437 (1943).
2. C.W. Tittle, Slow Neutron Detection by Foils, Part I, Nucleonics 8, No. 6, 5 (1951).
3. C.W. Tittle, Slow Neutron Detection by Foils, Part II, Nucleonics 9, No. 1, 60 (1951).
4. T.H.R. Skyrme, Reduction in Neutron Density Caused by an Absorbing Disc, MS-91 plus Appendix, (1943) (Manuscript, available at ORNL).
5. R.H. Ritchie and H.B. Eldridge, Thermal Neutron Flux Depression by Absorbing Foils, Nuclear Science and Engineering 8, No. 4, 300-311 (October, 1960). (Also by private communication)
6. John J. Kelly, Jr. and Neal W. Clements, Determination of Thermal Neutron Flux by Activation of a Pure Target with Known Cross Section, Thesis, US Naval Postgraduate School, June 1960.
7. R.L. Heath and F. Schroeder, The Qualitative Techniques of Scintillation Spectroscopy as Applied to the Calibration of Standard Sources, AEC Report IDO-16149 (1st rev) 1955.
8. R.L. Heath, Scintillation Spectrometry Gamma-Ray Spectrum Catalogue, AEC Report IDO-16408 (July, 1957).
9. J.F. Raffie, Determination of Absolute Neutron Flux by Gold Activation, J. Nuclear Energy, Part A: Reactor Science, Vol. 10, 1959.
10. A. Sola, Flux Perturbation by Detector Foils, Nucleonics 18, No. 3, 78 (1960).
11. W.H.B. Cooke (private communication in connection with an unpublished thesis, US Naval Postgraduate School, 1961.)
12. J.W. Meadows and J.F. Whalen, Thermal Neutron Absorption Cross Sections by the Pulsed Source Method, Nuclear Science and Engineering 9, No. 2, 132-136 (February, 1961).
13. C.H. Westcott, Effective Cross Section Values for Well-Moderated Thermal Reactor Spectra (3rd Edition), AECL-1101, Chalk River, Ontario (November 1, 1960).
14. W. Zobel, Experimental Determination of Flux Depression and Other Corrections for Gold Foils Exposed in Water, Trans. American Nuclear Society 3, No. 1, 168-169 (June, 1960). (Also private communication of revised results as yet unpublished).

15. D.R. Bach, et al, Low Energy Neutron Spectra Measurements in Polyethylene Moderated Media, (paper presented at the American Nuclear Society Meeting on December 14, 1960 at San Francisco, Calif.), Knolls Atomic Power Laboratory, Schenectady, N.Y.
16. G.R. Dalton and R.K. Osborn, Flux Perturbations by Thermal Neutron Detectors, Nuclear Science and Engineering 9, No. 2, 198-210 (February, 1961).
- Additional References of Interest
17. E.D. Klema and R.H. Ritchie, Phys. Rev. 87, No. 1, 167 (1952).
18. J. Bengston, Neutron self-shielding of a plane absorbing foil, CF-56-3-170 (1956).
19. W.J. Price, Nuclear Radiation Detection, McGraw-Hill, (1958), pages 53-66 and 285-289.
20. R.H. Ritchie, Thermal Neutron Flux Depression, Health Physics Division Annual Progress Report, O'NL-2806, 133 (July 31, 1959).
21. D. Martin, Correction Factors for Cadmium-Covered Foil Measurements, Nucleonics 13, No. 3, 52 (1955).
22. K.M. Case, F. deHoffman, and G. Placzek, Introduction to the Theory of Neutron Diffusion, Volume I, pages 153-156, US Government Printing Office, Washington, D.C., June, 1953.

APPENDIX I EXPERIMENTAL DATA

All data given below are expressed in terms of Channel Number on the 50 Channel Step-Scanning Spectrometer and in counts per minute for the gamma activity. The counting rate has been corrected for background as given on page 29. This background determination is the average of twenty separate counting runs made over a period of two weeks.

SAMPLE #1 - Two mills
February 7, 1961
Mass = 0.1273 gms.

Channel	Run No. 1	Run No. 2	Run No. 3
22	249	228	193
23	301	264	270
24	959	825	895
25	4193	3456	3561
26	9137	8111	7903
27	9656	9141	9355
28	4727	5087	4890
29	1179	1346	1258
30	167	187	203
31	75	75	93

SAMPLE #2 - Two mills
February 8, 1961
Mass = 0.1260 gms.

Channel	Run No. 1	Run No. 2	Run No. 3
22	178	191	181
23	281	234	226
24	967	748	614
25	3903	3250	2657
26	8691	7710	6963
27	8914	9516	9428
28	4223	5600	6114
29	922	1557	1779
30	142	254	285
31	47	69	61

24

SAMPLE #3 - Two mills
February 9, 1961
Mass = 0.1270 gms.

Channel	Run No. 1	Run No. 2	Run No. 3
22	323	203	203
23	446	309	279
24	1918	1217	1209
25	6625	4705	4404
26	10034	9221	9003
27	7651	8855	8988
28	2775	4189	4097
29	486	867	967
30	78	139	148

SAMPLE #4 - Two mills
February 10, 1961
Mass = 0.1160 gms.

Channel	Run No. 1	Run No. 2	Run No. 3
22	187	237	217
23	235	231	224
24	789	662	679
25	3310	2948	2808
26	7686	7083	7034
27	8964	8939	8911
28	4883	5281	5341
29	1239	1437	1547
30	163	209	250

SAMPLE #5 - Four Mills
February 13, 1961
Mass = 0.2543 gms.

Channel	Run No. 1	Run No. 2	Run No. 3
22	404	399	374
23	577	496	460
24	1967	1666	1674
25	7655	6851	6718
26	16250	15390	15048
27	16782	17113	17444
28	8364	8870	9340
29	2094	2287	2418
30	351	331	398
31	119	127	116

25

SAMPLE #6 - Four Mills
February 14, 1961
Mass = 0.2410 gms.

Channel	Run No. 1	Run No. 2	Run No. 3
22	188	178	155
23	227	184	190
24	560	511	499
25	2386	2260	2314
26	6092	6035	5933
27	8109	8051	8148
28	5004	4994	5317
29	1425	1409	1494
30	240	227	246
31	58	52	58

SAMPLE #7 - Four Mills
February 14, 1961
Mass = 0.2583 gms.

22	187	187	176
23	210	202	205
24	556	546	528
25	2283	2373	2247
26	8271	6341	6316
27	8585	8601	8510
28	5521	5631	5575
29	1697	1649	1635
30	264	277	279
31	46	71	58

SAMPLE #8 - Six Mills
February 15, 1961
Mass = 0.3931 gms.

23	236	248	202
24	919	738	711
25	3255	3121	2917
26	6976	6773	6610
27	7045	7233	7537
28	3414	3594	3667
29	751	951	865
30	114	138	143
31	44	51	39

SAMPLE #9 - Six Mills
February 15, 1961
Mass = 0.3814 gms.

Channel	Run No. 1	Run No. 2	Run No. 3
23	225	220	230
24	732	728	766
25	2940	3154	2852
26	6753	6738	6604
27	7383	7323	7328
28	3714	3646	3916
29	926	857	1014
30	124	125	143

SAMPLE #10 - Six Mills
February 15, 1961
Mass = 0.3974 gms.

23	199	221	234
24	748	650	737
25	2948	2694	2854
26	8881	6724	6688
27	7826	7753	7821
28	4311	4270	4242
29	1113	1022	1160
30	160	166	167

SAMPLE #11 - Eight Mills
February 16, 1961
Mass = 0.5044 gms.

22	191	206	155
23	325	260	269
24	1182	922	949
25	4864	3714	3350
26	7340	7184	6892
27	6468	6782	6594
28	2584	2823	2929
29	482	590	691
30	94	78	110

SAMPLE #12 - Eight Mils
February 16, 1961
Mass = 0.5234 gms.

Channel	Run No. 1	Run No. 2	Run No. 3
22	139	203	182
23	247	255	202
24	908	842	800
25	3313	3176	3145
26	7017	7020	6768
27	7118	7122	7121
28	3411	3391	3514
29	673	776	786
30	110	128	112

SAMPLE #13 - Eight Mils
February 16, 1961
Mass = 0.5285 gms.

22	194	221	182
23	247	259	223
24	849	851	854
25	3342	3249	3296
26	7024	6832	6916
27	7332	7118	7111
28	3445	3481	3412
29	702	735	746
30	110	128	112

SAMPLE #14 - Ten Mils
February 23, 1961
Mass = 0.6421 gms.

22	226	281	256
23	272	284	275
24	885	795	756
25	3182	3041	3039
26	7521	7231	7020
27	8420	8401	8377
28	4286	4717	4801
29	1126	1213	650
30	160	188	104

SAMPLE #15 - Ten Mils
February 23, 1961
Mass = 0.6300 gms.

Channel	Run No. 1	Run No. 2	Run No. 3
23	304	350	302
24	1219	1217	885
25	4233	4637	3567
26	8115	8546	7942
27	8408	7669	8377
28	3600	2822	4322
29	747	709	1196
30	120	141	158

SAMPLE #16 - Ten Mils
February 23, 1961
Mass = 0.6442 gms.

23	315	276	326
24	1055	1081	988
25	3815	3869	3803
26	7940	7861	7810
27	8138	8158	8010
28	3882	3997	4003
29	913	886	930
30	131	143	145

AVERAGE BACKGROUND

Channel	Counts per minute
20	27
21	26
22	27
23	24
24	26
25	25
26	23
27	22
28	22
29	22
30	19
31	17
32	17

APPENDIX II

Analysis of Peak-to-Total Ratio

One of the crucial correction factors in the determination of the absolute gamma emission rate is R_{pt} , the peak-to-total ratio used in the procedure given by Heath (8).

Referring to Figure 8, which is a numerical mean of the spectrum obtained throughout this investigation, it can be seen that the combined counts from backscatter, mercury x-rays, 0.680 mev Compton scattering, and 1.09 mev Compton scattering add up to introduce a significant error in peak-to-total ratio determination for the 0.411 mev peak if not taken into account.

A rough determination of this consideration yielded a value of $R_{pt} \approx 70\%$ which is in reasonable agreement with that determined by Heath (8). This compares with a value of 60% obtained from a comparison with window count in the spectrometer. Since Heath's investigation was carried out under more nearly ideal conditions, it was decided to use his value of R_{pt} which is 0.725.

30

END

10

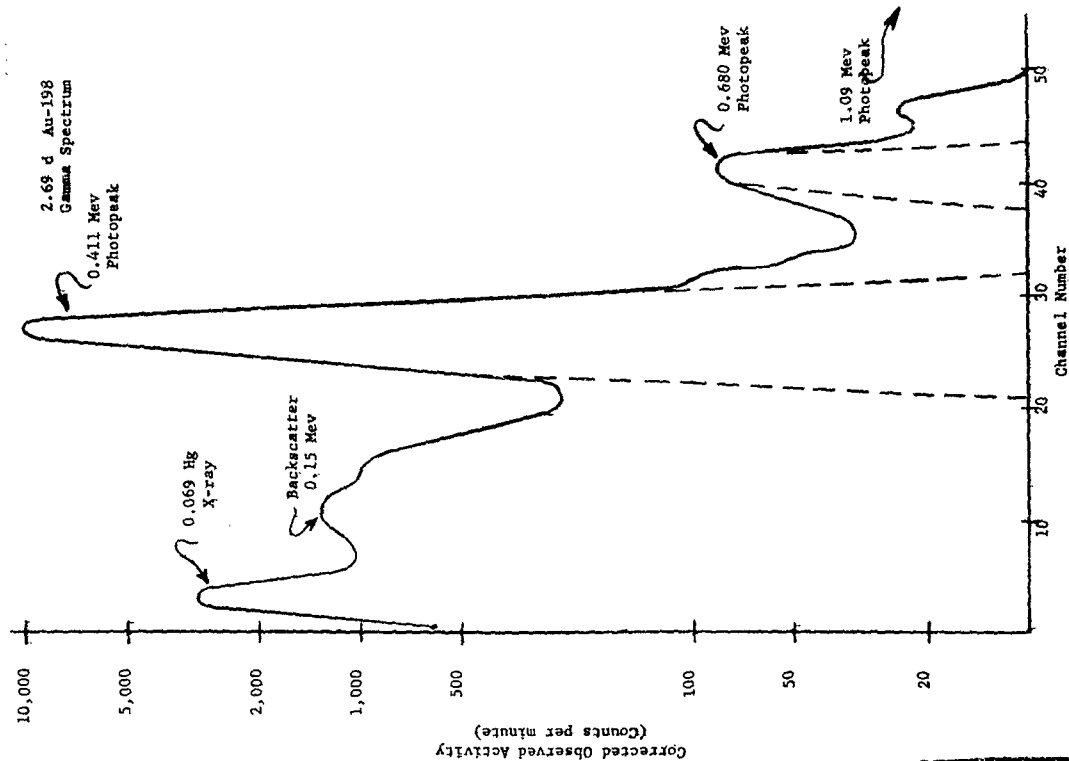


Figure 8

31